

A color-gradient-based phase-field equation for multiphase flow

Reza Haghani¹, Hamidreza Erfani¹, James E McClure², Eirik Grude Flekkøy³, Carl Fredrik Berg¹

¹PoreLab Center of Excellence, IGP, NTNU, Trondheim, Norway

²Advanced Research Computing, Virginia Tech, VA 24061, USA

³Physical Institute, Faculty of Mathematics and Natural Sciences, University of Oslo, Oslo, Norway



PoreLab
NTNU-UIO Porous Media Laboratory

Norwegian Centre of Excellence
The Research Council of Norway



Introduction

A phase-field interface-capturing model is proposed based on the well-known color-gradient (CG) model. The new formulation is developed for incompressible, immiscible two-fluid flows without phase-change phenomena, and a solver based on the lattice Boltzmann method is proposed. Coupled with an available robust hydrodynamic solver, a binary fluid flow package that handles fluid flows with high density and viscosity contrasts is presented. In contrast to existing color-gradient models where the interface capturing equations are coupled with the hydrodynamic ones and include the surface tension forces, the new formulation is in the same spirit as the other phase-field models such as the Cahn-Hilliard (CH) and the Allen-Cahn (AC) equations and is solely employed to capture the interface advected due to a flow velocity. As such, similar to other phase-field models, a mobility parameter comes into play which is not related to the density field but is a constant coefficient. The present model has been tested to handle complex fluid flows with density and viscosity ratios of 1000 and 100, respectively.

Numerical Methods

We first develop a new phase-field formulation based on the CG model. Then, a LB model is developed which comprises three distinct distribution functions. Two of these are employed to recover the macroscopic interfacial evolution equations, while the last one is utilized to recover the hydrodynamic properties. The original CG equations are:

$$\begin{aligned} \frac{\partial \tilde{\rho}_r}{\partial t} + \nabla \cdot (\mathbf{u} \tilde{\rho}_r) &= D \nabla^2 \tilde{\rho}_r - D \frac{4}{W} \nabla \cdot \left[\frac{\tilde{\rho}_r \tilde{\rho}_b}{\tilde{\rho}_r + \tilde{\rho}_b} \mathbf{n} \right] \\ \frac{\partial \tilde{\rho}_b}{\partial t} + \nabla \cdot (\mathbf{u} \tilde{\rho}_b) &= D \nabla^2 \tilde{\rho}_b + D \frac{4}{W} \nabla \cdot \left[\frac{\tilde{\rho}_r \tilde{\rho}_b}{\tilde{\rho}_r + \tilde{\rho}_b} \mathbf{n} \right] \end{aligned} \quad (1)$$

By defining the order parameter as $\phi_i = \frac{\tilde{\rho}_i}{\rho_i}$ (subscript $i=r$ or b represents the *red* or *blue* fluid), we have

$$\begin{aligned} \frac{\partial \phi_r}{\partial t} + \nabla \cdot (\mathbf{u} \phi_r) &= D \nabla^2 \phi_r - D \frac{4}{W} \nabla \cdot \left[\frac{\phi_r \phi_b}{\phi_r \left(\frac{\rho_r}{\rho_b} \right) + \phi_b} \mathbf{n} \right] \\ \frac{\partial \phi_b}{\partial t} + \nabla \cdot (\mathbf{u} \phi_b) &= D \nabla^2 \phi_b + D \frac{4}{W} \nabla \cdot \left[\frac{\phi_r \phi_b}{\phi_r + \phi_b \left(\frac{\rho_b}{\rho_r} \right)} \mathbf{n} \right] \end{aligned} \quad (2)$$

Here one can assure the density ratio is one, calculate the order parameters, and then calculate the density through:

$$\rho = \phi_r \rho_r + \phi_b \rho_b \quad (3)$$

The following relation defines a new order parameter deciding the location of the interface:

$$\phi = \frac{1}{2} \left[\frac{\phi_r - \phi_b}{\phi_r + \phi_b} + 1 \right] \quad (4)$$

The above equations and the hydrodynamic equations are solved based on lattice Boltzmann models and the details of the models can be found in [1] and [2].

Results

To assess the accuracy of stability of the proposed model, different benchmarks are conducted. In the first four tests, we only consider the interface evolution equations alone, and so the velocity field is prescribed. In the rest of the tests, the hydrodynamic equations are also solved and coupled with the interface evolution equations through the order parameter and the velocity field.

□ Diagonal translation of circular interfaces

A circular droplet is placed in the middle of a square domain (periodic boundary condition) with the following velocity field prescribed:

$$\begin{aligned} u_x &= U_0 \\ u_y &= U_0 \end{aligned}$$

The circular returns to its original configuration after one period.

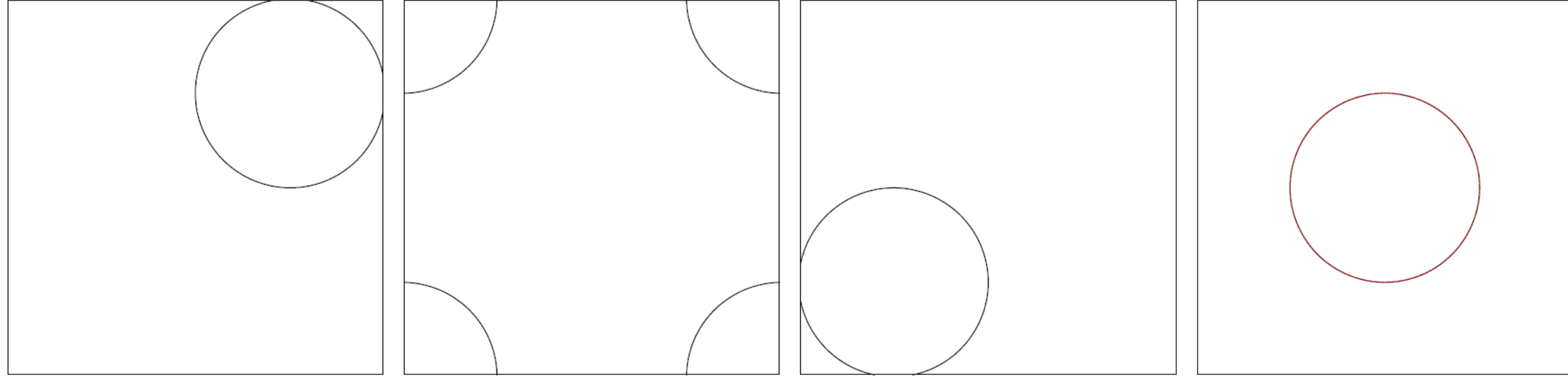


Fig. 1: Diagonal translation of a circular interface at $Pe = WU_0/D = 60$ and $Ch = W/L_0 = 3/100$.

□ Rotation of Zalesak's disk

A circular disk with a slot placed at the center of a square domain with the following vortex flow:

$$\begin{aligned} u_x &= -U_0 \pi \left(\frac{y}{L_0} - 0.5 \right) \\ u_y &= U_0 \pi \left(\frac{x}{L_0} - 0.5 \right) \end{aligned}$$

The circular returns to its original configuration after a complete rotation.

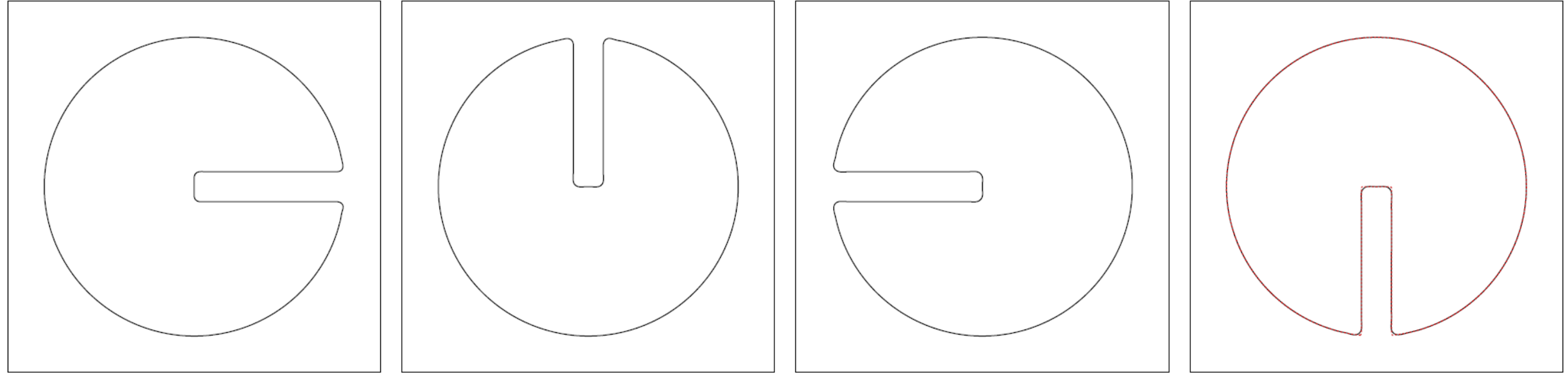


Fig. 2: Rotation of Zalesak's disk at $Pe=60$ and $Ch=3/200$.

□ Circular interface in a shear flow

A circular interface is placed on the middle bottom of a square domain with the following shear flow which is reversed at the middle of the simulation:

$$\begin{aligned} u_x &= -U_0 \pi \cos \left[\pi \left(\frac{x}{L_0} - 0.5 \right) \right] \sin \left[\pi \left(\frac{y}{L_0} - 0.5 \right) \right] \\ u_y &= U_0 \pi \sin \left[\pi \left(\frac{x}{L_0} - 0.5 \right) \right] \cos \left[\pi \left(\frac{y}{L_0} - 0.5 \right) \right] \end{aligned}$$

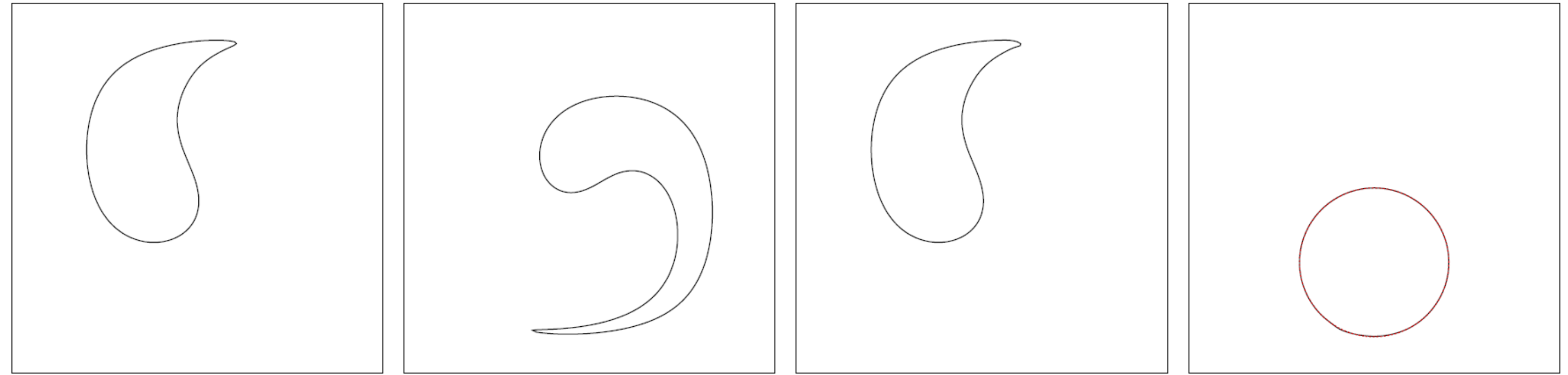


Fig. 3: Circular interface in a shear flow at $Pe=60$ and $Ch=3/200$.

□ Deformation of a circular interface

A circular interface experiences large topological changes as:

$$u_x = -U_0 \sin \left[4\pi \left(\frac{x}{L_0} + 0.5 \right) \right] \sin \left[4\pi \left(\frac{y}{L_0} + 0.5 \right) \right] \cos \left[\frac{\pi t}{t_0} \right]$$

$$u_y = U_0 \cos \left[4\pi \left(\frac{x}{L_0} + 0.5 \right) \right] \cos \left[4\pi \left(\frac{y}{L_0} + 0.5 \right) \right] \cos \left[\frac{\pi t}{t_0} \right]$$

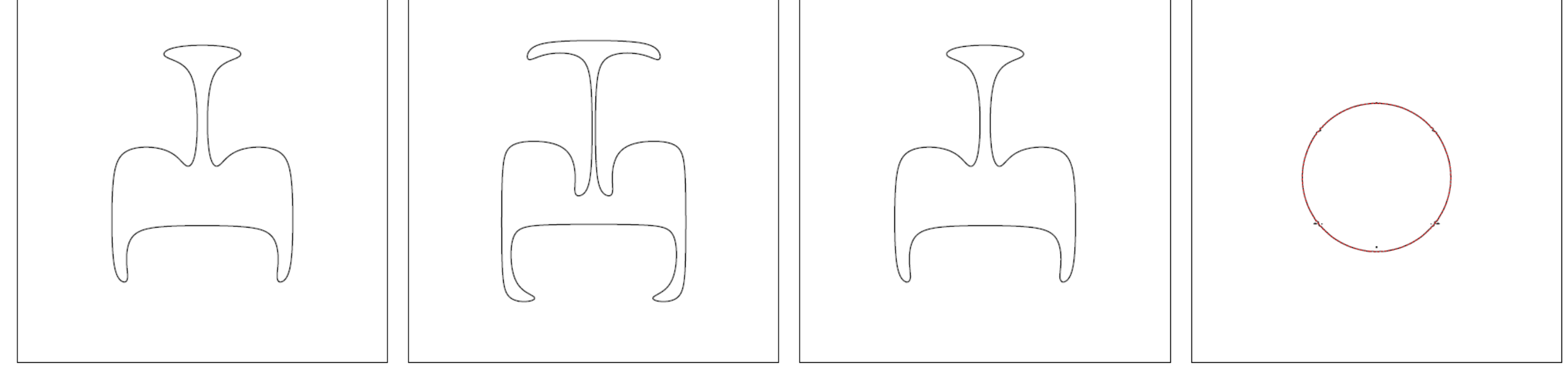


Fig. 5: Smoothed deformation of a circular interface at $Pe=60$ and $Ch=3/500$.

□ Laplace test

The hydrodynamic equation is solved for the rest of benchmarks with systems with density and viscosity ratios of 1000 and 100, respectively. First the Laplace test is conducted. For a zero surface tension, the present model does not produce spurious velocities in contrast to other CG models [3].

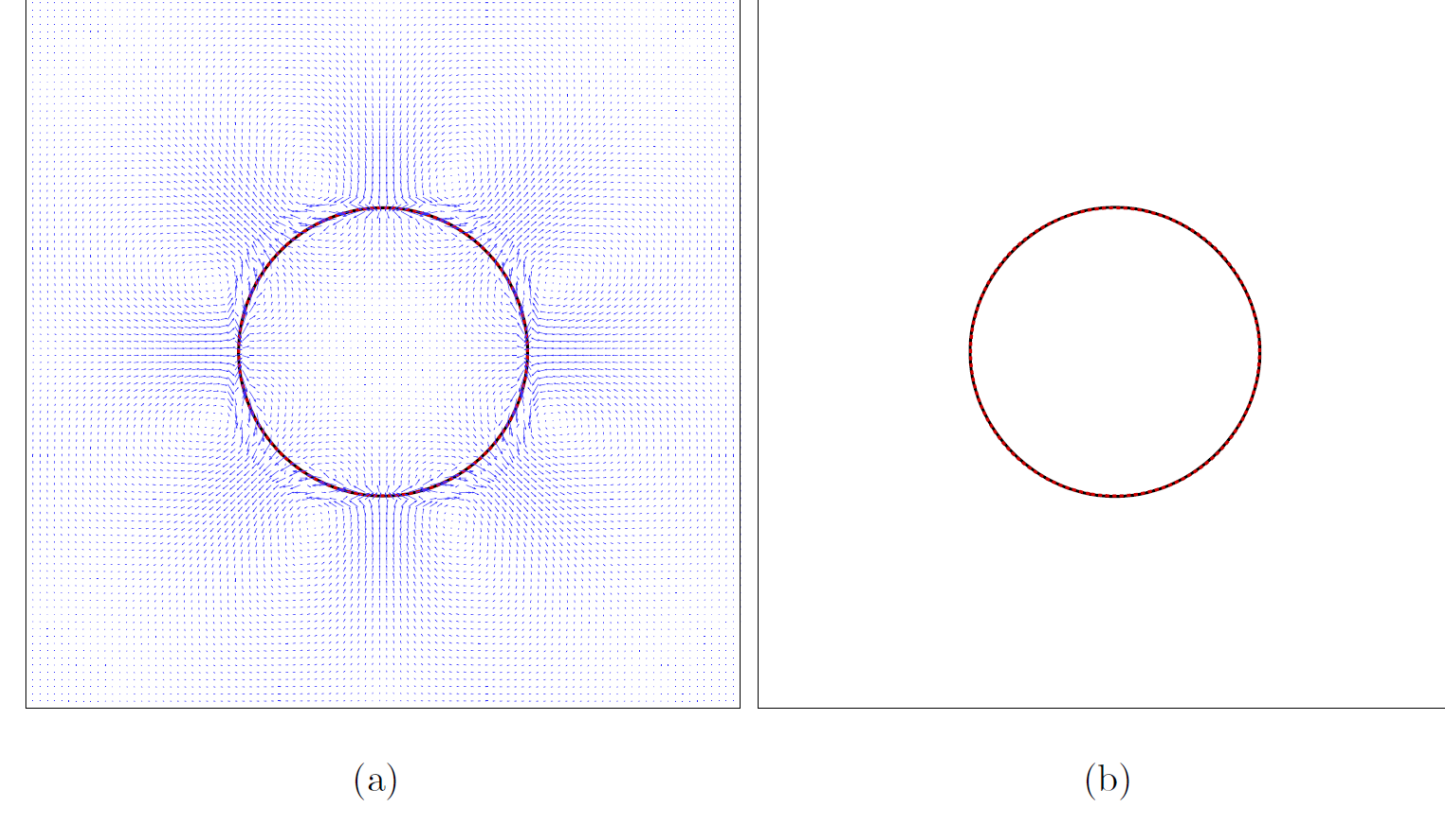


Fig. 6: Parasite currents for the Laplace test for density ratio $\rho^* = \rho_r/\rho_b = 1000$ and dynamic viscosity ratio $\eta^* = \eta_r/\eta_b = 100$. (a) $\sigma = 0.001$ and (b) $\sigma = 0$.

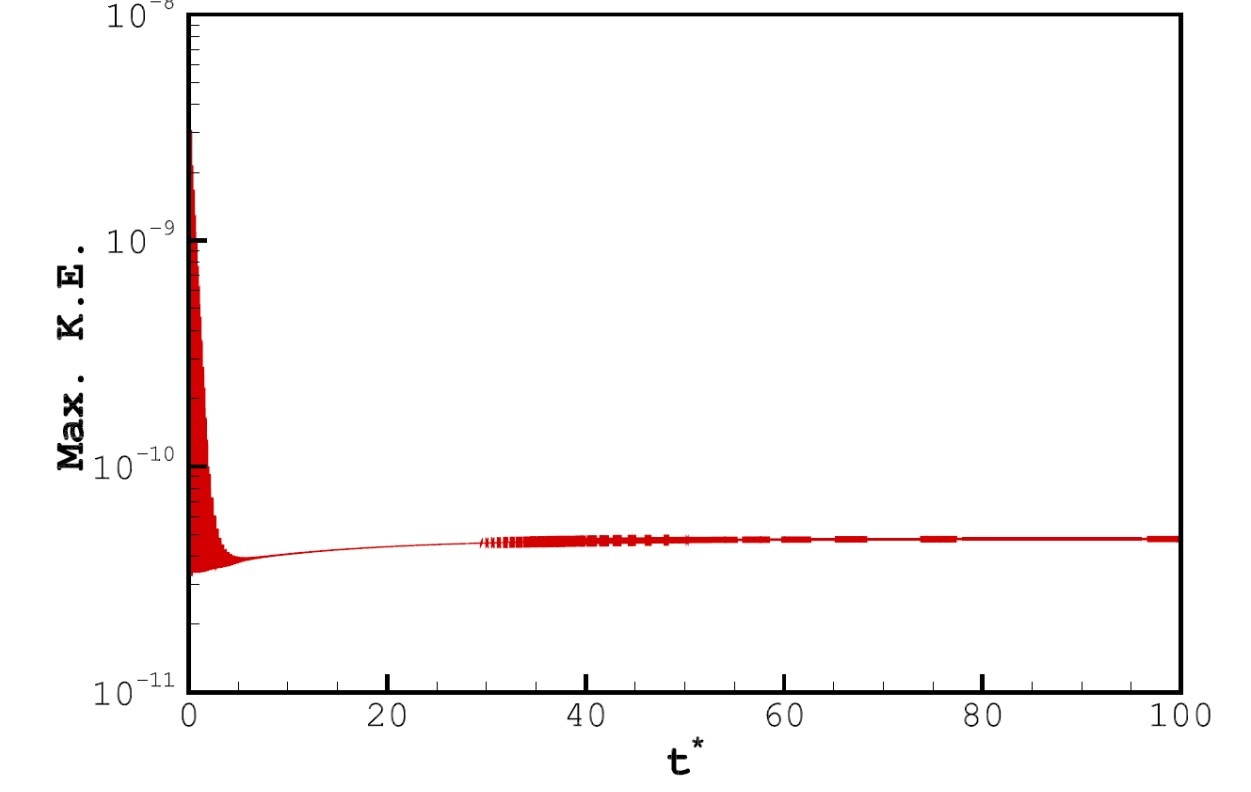


Fig. 7: Maximum kinetic energy for $\rho^* = 1000$ and $\eta^* = 100$. $\sigma = 0.001$.

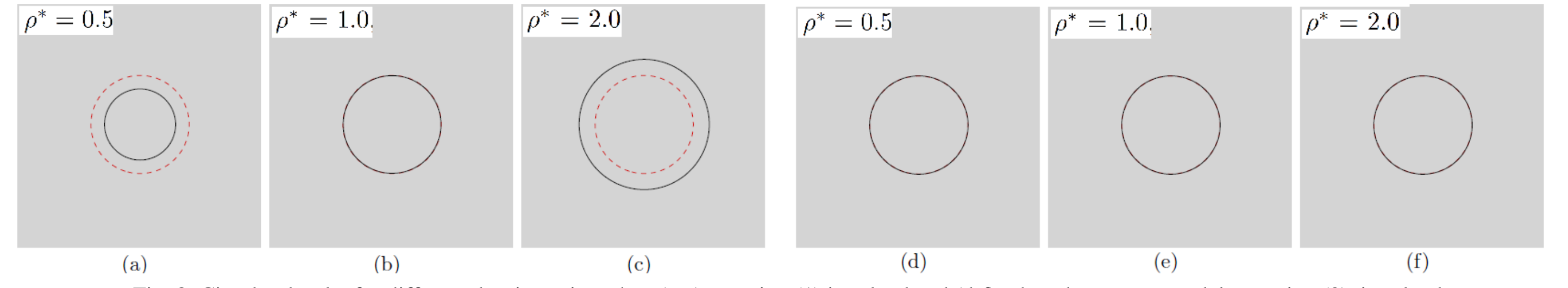


Fig. 8: Circular droplet for different density ratios when (a-c) equation (1) is solved and (d-f) when the present model, equation (2), is solved.

□ Rayleigh-Taylor instability (RTI)

A layer of heavy fluid lies above a lighter fluid in a gravitational field. A strong enough perturbation at the interface results in the replacement of the two fluids. The phase field domain for two different sets of dimensionless parameters are shown.

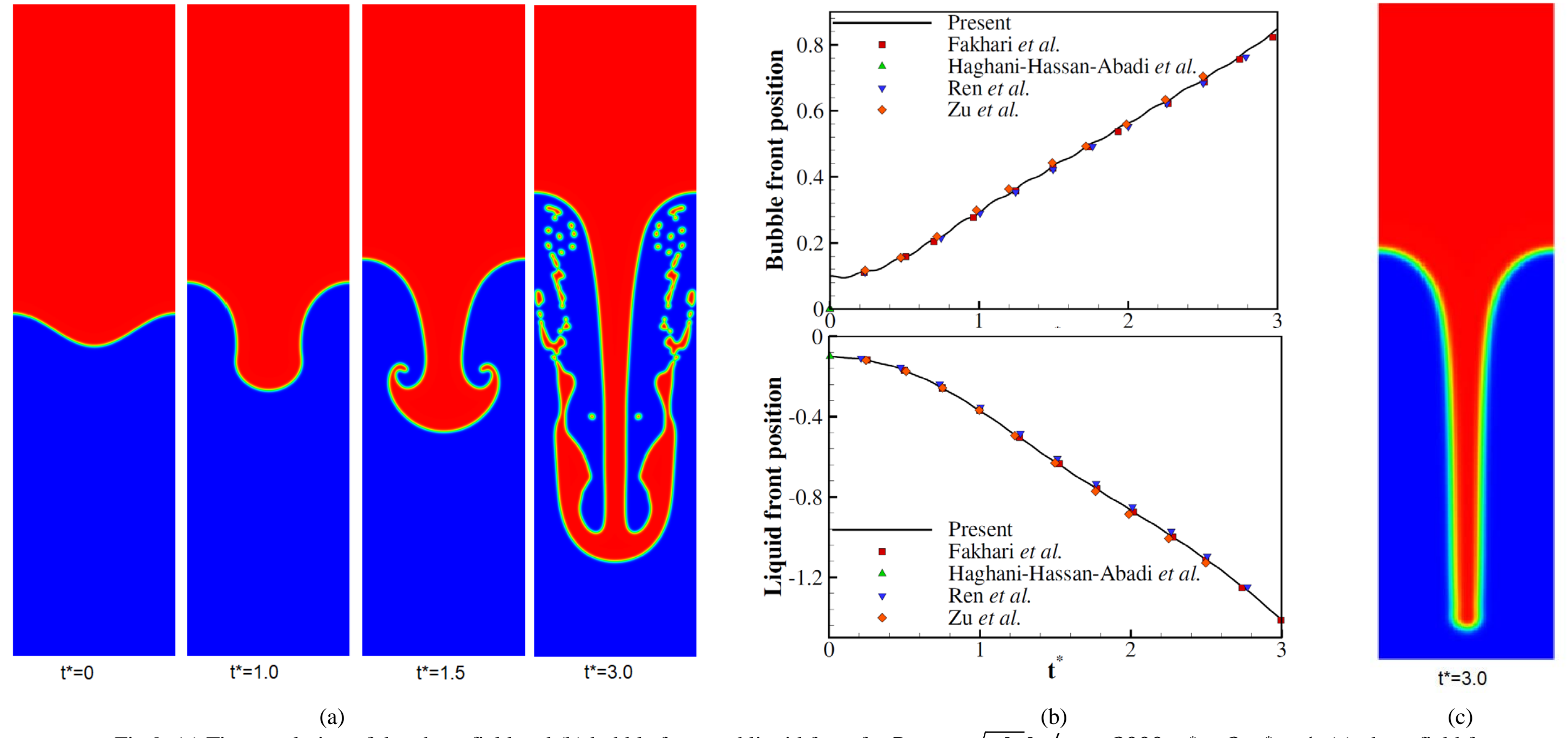


Fig 9: (a) Time evolution of the phase field and (b) bubble front and liquid front for $Re = \rho_r \sqrt{g L_0} / \eta_r = 3000$, $\rho^* = 3$, $\eta^* = 1$. (c) phase field for $Re=3000$, $\rho^* = 1000$, $\eta^* = 100$.

□ Droplet splashing on a thin liquid film

Finally, a droplet splashing on a thin liquid film is conducted. The dimensionless parameters are $We = \frac{2\rho_r U_0^2 R}{\sigma} = 8000$, $Re = \frac{2\rho_r U_0 R}{\eta_r} = 500$, $\rho^* = 1000$, $\eta^* = 100$.

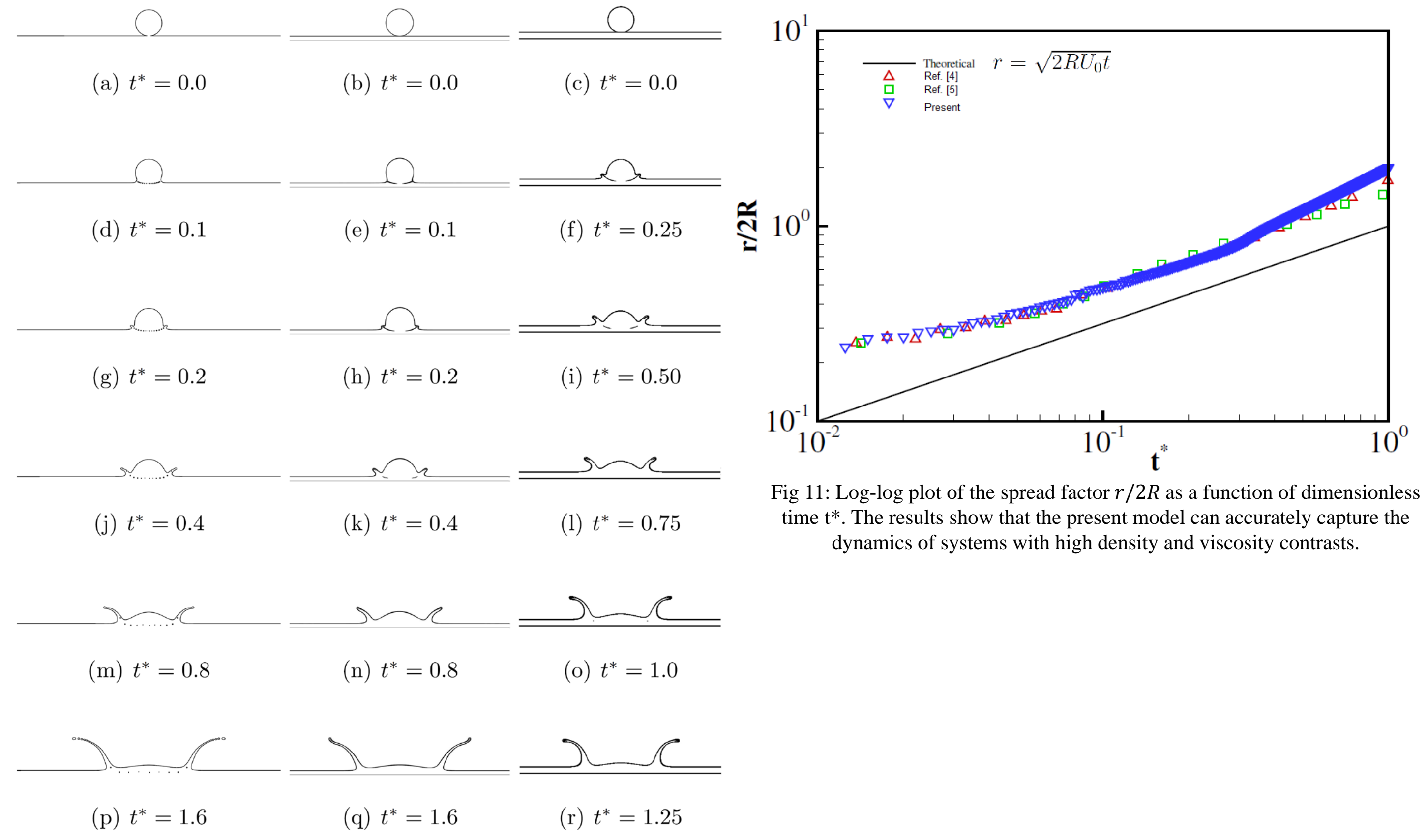


Fig 10: Droplet splashing on a thin film. Left frames: the present models, middle frames: Ref [4], right frames: Ref. [5].

References

- 1- Haghani-Hassan-Abadi, Reza, Mohammad-Hassan Rahimian, and Abbas Fakhari. "Conservative phase-field lattice-Boltzmann model for ternary fluids." *Journal of Computational Physics* 374 (2018): 668-691.
- 2- Haghani-Hassan-Abadi, Reza, Abbas Fakhari, and Mohammad-Hassan Rahimian. "Phase-change modeling based on a novel conservative phase-field method." *Journal of Computational Physics* 432 (2021): 110111.
- 3- Akai, B. Bijeljic, M. J. Blunt, Wetting boundary condition for the color-gradient lattice Boltzmann method: Validation with analytical and experimental data, *Advances in Water Resources* 116 (2018) 56–66.
- 4- T. Lee, C.-L. Lin, A stable discretization of the lattice Boltzmann equation for simulation of incompressible two-phase flows at high density ratio, *Journal of Computational Physics* 206 (2005) 16–47.
- 5- J. Y. Shao, C. Shu, A hybrid phase field multiple relaxation time lattice Boltzmann method for the incompressible multiphase flow with large density contrast, *International Journal for Numerical Methods in Fluids* 77 (2015) 526–543.